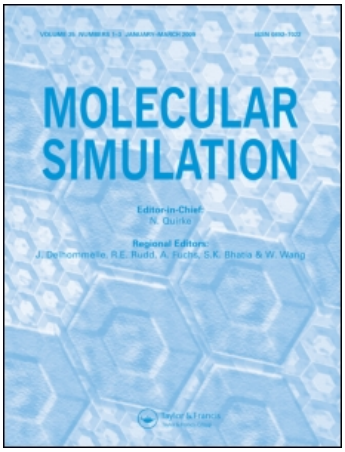

Molecular Simulation
Publication details, including instructions for authors and subscription information:
http://www.informaworld.com/smpp/title~content=t713644482

Molecular Dynamics Study of Li_2SiO_3 in the Liquid and Glassy States

Junko Habasaki[a]; Isao Okada[a]
[a] Department of Electronic Chemistry, Tokyo Institute of Technology at Nagatsuta, Yokohama, Japan

To cite this Article Habasaki, Junko and Okada, Isao(1992) 'Molecular Dynamics Study of Li_2SiO_3 in the Liquid and Glassy States', Molecular Simulation, 8: 3, 179 — 195
To link to this Article: DOI: 10.1080/08927029208022475
URL: http://dx.doi.org/10.1080/08927029208022475

Molecular Simulation, 1992, Vol. 8, pp. 179–195
Reprints available directly from the publisher
Photocopying permitted by license only

MOLECULAR DYNAMICS STUDY OF Li_2SiO_3 IN THE LIQUID AND GLASSY STATES

JUNKO HABASAKI and ISAO OKADA

Department of Electronic Chemistry, Tokyo Institute of Technology at Nagatsuta, Nagatsuta, Yokohama, Japan

(*Received January 1991, accepted June 1991*)

Molecular dynamics simulation (MD) has been carried out for Li_2SiO_3 in the molten and glassy states. The parameters of the pair potential functions were determined by a trial and error method so that the results of X-ray diffraction analysis could be well reproduced.

The changes in the structure and dynamic properties accompanied by lowering temperature revealed that the glass transition of this simulated system occurred between 973 and 700 K. The ratio of the bridging oxygens to non-bridging oxygens was nearly constant over the investigated temperature range, while a small change in the pattern of branching of the -Si-O- framework was found. The second peaks in the pair correlation functions $g_{Si-O}(r)$ and $g_{Si-Si}(r)$ split at lower temperature. These splittings suggest that the motion changing the relative orientations of two neighboring SiO_4 units may be nearly frozen at lower temperature.

KEY WORDS: MD simulation, lithium silicate, structure, melt, glass

1 INTRODUCTION

Alkali silicates are important not only for practical use but also for a better understanding of a glassy state. The three dimensional structure of glasses, however, has not fully been elucidated. Although many molecular dynamics (MD) studies on the glass transition have been performed for simple systems such as argon, the structural change in the glass transition has scarcely been studied for silicate systems. In this work, Li_2SiO_3 system is chosen as a model of glass forming systems. Attention was mainly focused on the structural differences between the melt and the glass in the Li_2SiO_3 system in the short and medium range, as there is no long range order in glassy state. This simulation should be treated as a "computer experiment" at short times because of a very rapid cooling schedule, in which direct comparison with other experimental results is difficult. As for the long range structure, such as framework composed of SiO_4 units, it could not be considered to be at equilibrium at the present rapid cooling rate.

2 METHOD

Molecular dynamics simulation has been performed for Li_2SiO_3 in a similar manner as in a previous study [1]. Pair potentials of the Gilbert–Ida type [2] were used:

$$\psi_{ij} = z_i z_j e^2/r + f_0(b_i + b_j) \exp\{(a_i + a_j - r_{ij})/(b_i + b_j)\} - c_i c_j/r^6, \quad (1)$$

where z is the effective charge number, e the elementary charge; a, b and c are the parameters characteristic of the atoms; f_0 is a nomalization constant (4.184 kJ Å^{-1} mol^{-1}). The parameters were determined by a trial and error method so that the results from X-ray diffraction [3] were well reproduced. The parameters thus adopted are given in Table 1. The positions of the first peak of the pair correlation function $g(r)$ at 1673 K and 500 K are given in Table 2 in comparison with those obtained by X-ray [3, 4] and neutron diffractions [3, 5]. The agreement for the peak positions between the MD and the experiments is good. Nearly tetrahedral SiO_4 units were kept during the MD-run.

The system was equilibrated at 4000 K during a more than 10 000 time-step run starting from a random configuration. Then, the system was cooled down in the following way. Chosen temperatures were 3000 K, 2000 K, 1673 K, 1173 K, 973 K, 700 K, 500 K and 300 K. Step-times of 1 fs (from 4000 to 2000 K) and 4 fs (from 1673

Table 1 Parameters of the potentials used in this work.

Ion	z	c/Å^3 kJ$^{1/2}$ mol$^{-1/2}$	a/Å	b/Å
O	−1.40	54.0	1.81	0·142
Si	2.60	0	0.75	0·036
Li	0.80	0	0·85	0·040

Table 2 Characteristic values of the first peak of pair correlation functions, $g(r)$.

	r/Å					
	Li–Li	Si–Si	O–O	Li–Si	Li–O	Si–O
1673 K*						
r_{max}	2.77	3.15	2.62	3.17	2.00	1.59
r_2	3.57	3.36	2.88	3.74	2.46	1.81
r_{min}	4.31	3.63	3.01	4.27	2.75	2.15
500 K*						
r_{max}	2.57	3.10	2.60	3.01	2.01	1.59
r_2	3.45	3.28	2.83	3.53	2.33	1.72
r_{min}	3.45	3.39	2.87	3.95	2.71	1.89

*this work.

X-ray diffraction analysis

System	r/Å				
	O–O	*Si–Si*	*Li–O*	*Si–O*	
Li_2O–$2SiO_2$ melt	2.66	3.13	2.08	1.61	[3]
Li_2O–$2SiO_2$ glass	2.65	3.13	2.07	1.62	[3]
Li_2O–SiO_2 glass			2.21	1.61	[4]

Neutron diffraction analysis

System	r/Å				
	O–O	*Si–Si*	*Li–O*	*Si–O*	
Li_2O–$2SiO_2$ glass	2.65		2.0	1.624	[5]
Li_2O–$2SiO_2$ glass	2.65	3.15	2.07	1.62	[3]

to 300 K) were used. The velocities of all the particles were set as zero at the beginning of the run at each temperature. A modified Woodcock method [6] was employed to achieve a desired temperature for about 200 steps. The configurations in the subsequent 2000 steps at a constant energy run were used for analysis. The volume at each temperature was obtained by interpolating the data [7] on the density of the melt and the glass. The run at 500 K was continued further 6000 steps to confirm a stability of the structure achieved by rapid quenching.

3 RESULTS AND DISCUSSION

3.1 *Glass Transition*

3.1.1 *Self-diffusion coefficients and mean square displacements*

The logarithmic values of the self-diffusion coefficients D obtained by Einstein's equation are plotted against $1/T$ in Figure 1. In laboratory glasses, the slope of log D vs. $1/T$ changes at the glass transition temperature. It is difficult to determine the

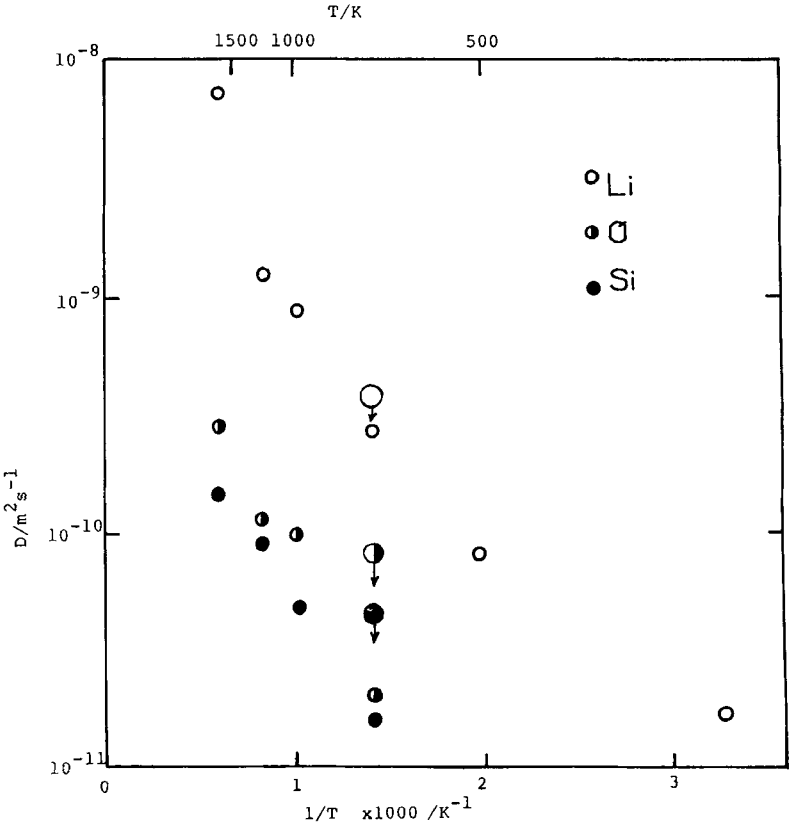

Figure 1 Temperature dependence of self-diffusion coefficients. At 700 K, two values are plotted for each atom; the larger ones and the smaller ones are calculated for the first 1000 steps and the subsequent 1000 steps, respectively.

exact values of D in a lower temperature region especially for silicon and oxygen because of the small root mean square displacements within an 8 ps run. The change in the slope for lithium was observed between 973 and 700 K, and the two points for each atom at 700 K in Figure 1, corresponding to the results derived from the first 1000 steps and the subsequent 1000 steps, show time dependent characters. The structural change observed during this period is described in a separate paper [8].

These findings are similar to the results obtained by Soules and Busbey for the Na_2O–SiO_2 system [9]. They argued that in a rapid cooling rate, the structure is frozen in at a fictive temperature much higher than the laboratory glass transition temperature and the glass transition range is smeared out compared to that found in laboratory glasses. At a rapid cooling rate, not all structure observed is at equilibrium as they point out. However, some parts of the structure in the short and medium range can be considered to be at local equilibrium if the relaxation time of the changes for the local structures is rapid enough. For example, the heights of the first peaks of the pair distribution functions take characteristic values for the respective temperature within the *ca.* 200 steps at constant temperature conditions, in this work. Thus, as far as the short range is concerned, the structure in the glassy state does not show hysteresis and therefore the glass transition range does not smear out.

The diffusion coefficients obtained from the data of further 6000 steps run at 500 K become less than 9×10^{-12} m^2/s for Li. The time dependence of the dynamics is one of the characteristics of the simulated glass in vicinity of the glass transition temperature. A further study of the dynamics of atoms in the glassy state during a longer period is in progress [10].

Mean squared displacements of the atoms within 3 ps are plotted in Figure 2. Below 973 K the values for the silicon and oxygen atoms converge to small values comparable to the magnitude of vibration at stable sites; therefore, the glass transition range in this simulation is inferred to be between 973 and 700 K. The observed glass

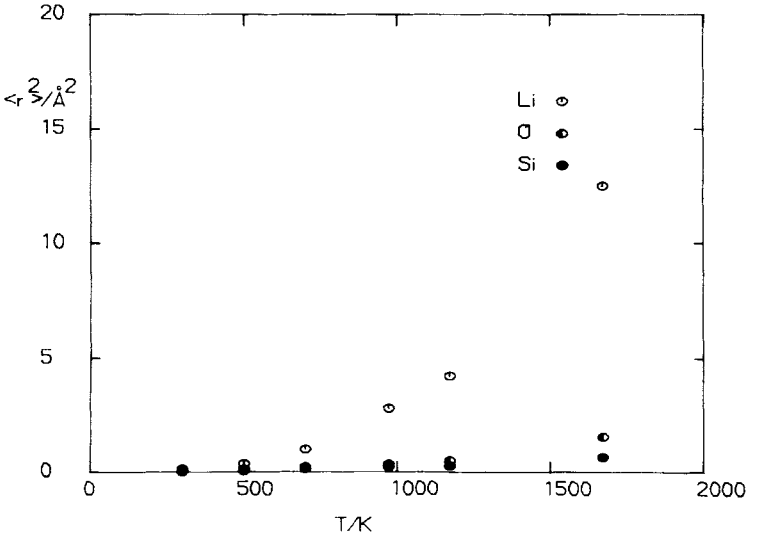

Figure 2 Mean squared displacements in a 3 ps run.

transition temperature is slightly higher than the experimental one, 687 K [11]. The higher value may be due partly to the restricted cell size and partly to the used pair potentials.

3.1.2 *Pair distribution functions*

The pair distribution functions $g(r)$ at 1673 K, 973 K and 500 K are shown in Figure 3. The heights of the first peak of the $g(r)$'s are plotted against temperature in Figure 4.

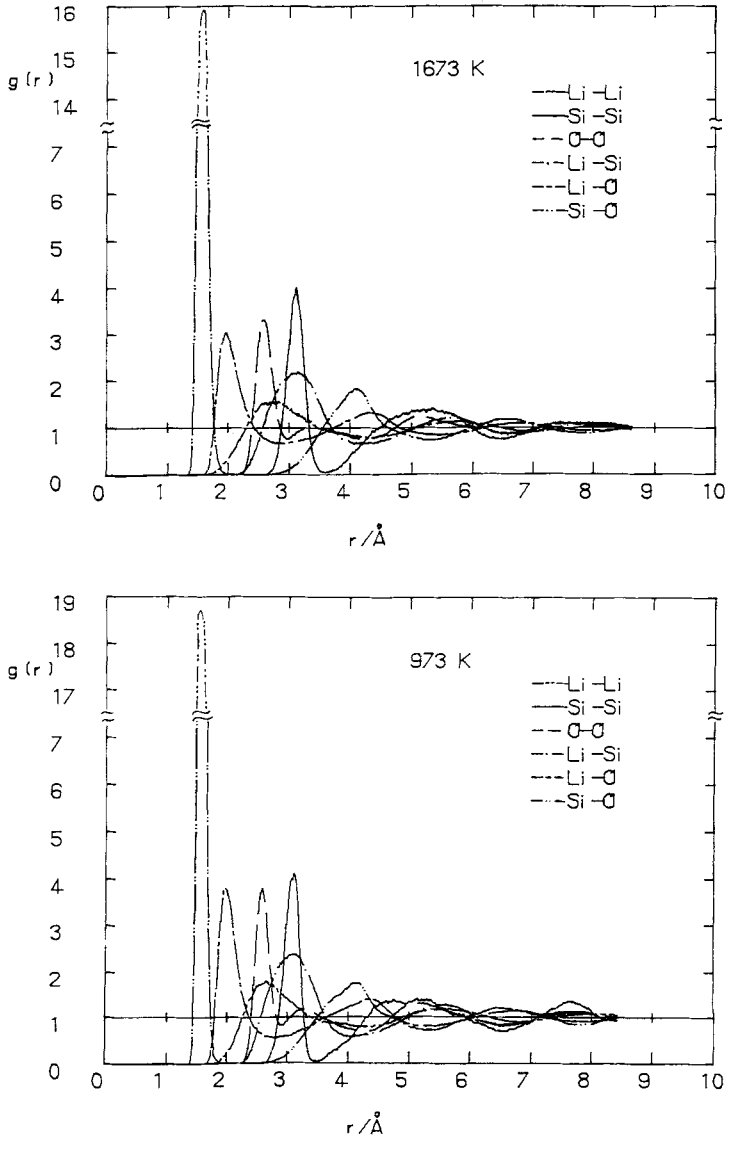

Figure 3 Pair distribution functions at 1673 K, 973 K and 500 K (a: 1–1000, b: 7001–8000 steps at a constant energy condition).

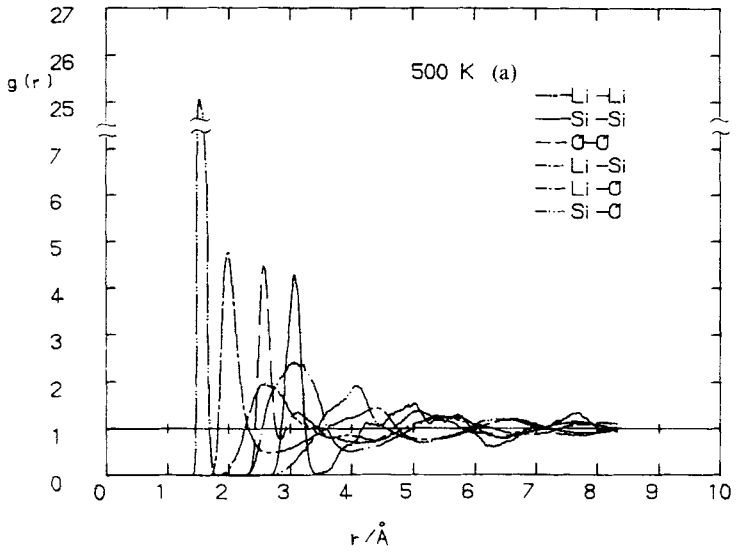

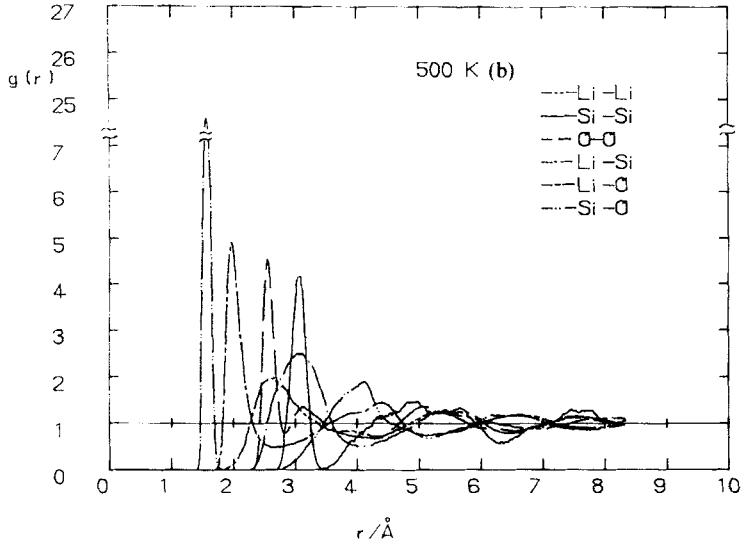

Figure 3 Cont.

There seems to exist an inflection point around 900 K particularly for the pairs involving oxygen, i.e., $g_{Si\text{-}O}(r)$, $g_{O\text{-}O}(r)$ and $g_{Li\text{-}O}(r)$. This inflection point suggests that the structure at short range, which is related to the packing of oxygen atoms, changes at around this temperature. The change also suggests that the glass transition point is between 973 K and 700 K, as similar changes in pair distribution functions at the glass transition are well known in many systems. Other evidence of glass formation will be given elsewhere [10].

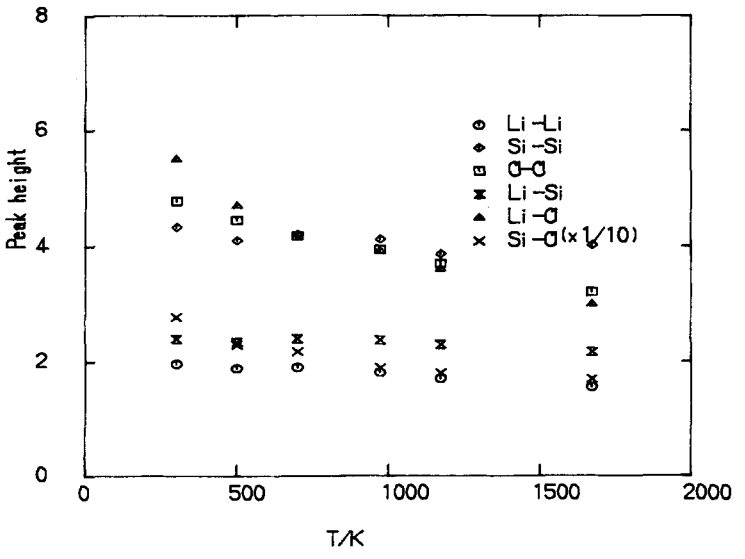

Figure 4 Temperature dependence of the heights of the first peak of the pair correlation functions.

The splitting of the second peaks of $g(r)$ for Si–O and for Si–Si pairs at the lower temperature is characteristic change around the glass transition temperature, which will be discussed later.

Since there are no remarkable changes in $g(r)$s at 500 K during an 8000 steps run in constant energy condition (see Figure 3), a local equilibrium of the structure is inferred to be nearly attained during the 200 steps run at constant temperature.

3.1.3 *Framework structures*

The system contains chains and rings made of SiO_4 units at all the temperatures. Examples of linkage of units (–Si–O–Si–) in the MD basic cell at an arbitrarily chosen step at 1673 K and 700 K are depicted in Figure 5, where the distance corresponding to r_{min} for g_{Si-O} is regarded as the limiting distance for bonding; r_{min} is the distance at the first minimum of $g(r)$. The size of the chains and rings may depend on the size of the MD cell and also on the initial configuration under inevitably limited time evolution.

The temperature dependence of the coordination numbers of silicon atoms about an oxygen atom have been examined to determine the change in the framework structure around the glass transition temperature. The coordination numbers of Si about O within r_{min} are shown in Table 3, which reveals that at this cooling rate the ratio of bridging and non-bridging oxygen atoms does not appreciably change at the glass transition point. Therefore, development of the bridging is not the cause of the glass transition observed here, although this may occur during relaxation of the glass on a much longer time scale.

The distribution of the coordination numbers of silicon atoms about a silicon atom is listed in Table 4. The r_{min} for g_{Si-Si} is taken here as a cutoff distance. The numbers thus counted indicate a feature of the linkage of the SiO_4 units.

1673 K

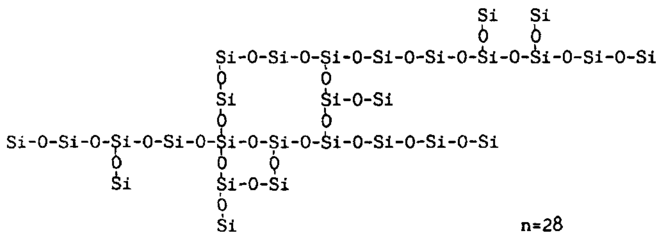

n=28

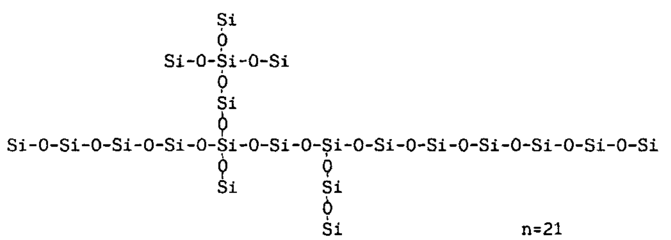

n=21

n	1	2	3	4	5	6	7	8	21	28
	6	3	0	1	0	0	1	0	1	1

700 K

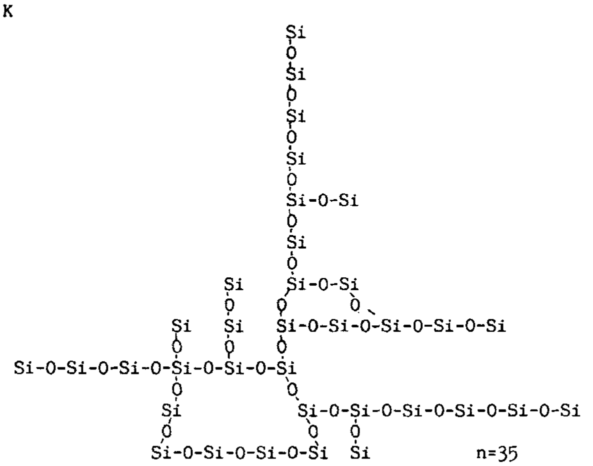

n=35

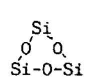

n=3

n	1	2	3	4	5	6	7	35
	11	2	4	0	2	0	0	1

Figure 5 Some examples of linkage of SiO_4 units in an arbitrarily chosen step at 1673 K and 700 K. The number of SiO_4 units in linkage is given in the tables.

Table 3 Temperature dependence of the distribution of the coordination numbers of silicon atoms (%) about an oxygen atom.

T/K	*n*			*Mean*
	0	*1*	*2*	
1673	4.17	58.33	37.50	1.33
1173	3.24	60.60	36.15	1.33
973	3.24	60.19	36.57	1.33
700	3.24	60.19	36.57	1.33
500	3.24	60.19	36.57	1.33
300	3.24	60.19	36.57	1.33

Table 4 Temperature dependence of the distribution of the coordination numbers of silicon atoms (%) about a silicon atom.

T/K	*n*					*Mean*
	0	*1*	*2*	*3*	*4*	
1673	0.00	16.81	48.40	27.78	7.01	2.25
1173	4.24	15.42	41.39	31.74	7.22	2.22
973	4.17	15.28	42.78	31.81	5.97	2.20
700	4.30	15.56	42.57	31.94	5.62	2.19
500	4.24	15.28	42.85	31.94	5.69	2.20
300	4.31	15.28	42.92	31.94	5.56	2.19

During cooling from 1673 K to 1173 K, the percentages of coordination numbers $n = 1$ and $n = 2$ decrease and those of $n = 0$ and 3 increase. This change in the pattern concerned with the connection of SiO_4 units occurs in the supper-cooled liquid region, and is not observed in a fast cooling proces ($\sim 2 \times 10^{15}$ K/s). Therefore, the fluctuation of the density of SiO_4 units in the glassy state is considered to become larger in a slower cooling process.

3.2 *Local Structures of Chains*

3.2.1 *Splitting in the second peak of $g_{Si\text{-}O}(r)$ and of the angular distributions Si–O–Si*

The angular distributions of $\angle Si_i$–O–Si_j at 1673 K and 500 K are shown in Figure 6. The angular distribution function $P(\theta)$ is defined by Equation (2)

$$P(\theta) = Cdn(\theta)/d\theta \tag{2}$$

where $dn(\theta)$ is the number of the triplets in which $\angle$Si–O–Si is between θ and $\theta + d\theta$ and Si–O distance is below 4.5 Å, where g_{Si} approximately crosses unity after the second peak. Then the component of the broad peak around 45° corresponds to the second peak component of the $g_{Si\text{-}O}(r)$. C is a normalization constant taken so that $\int_{0°}^{180°} P(\theta)d\theta = 1$ for the bridging oxygens, and the peak positions sifts from *ca.* 150° to 140° with a volume change accompanied by lowering temperature.

The peak around 45° becomes more asymmetric with decreasing temperature; the peak can be divided into two components. The narrower one is due to the oxygens connecting with neither Si_i nor Si_j, and the broader one is for the oxygens connecting with either Si_i or Si_j. The latter has a single peak at 1673 K, while it has a shoulder

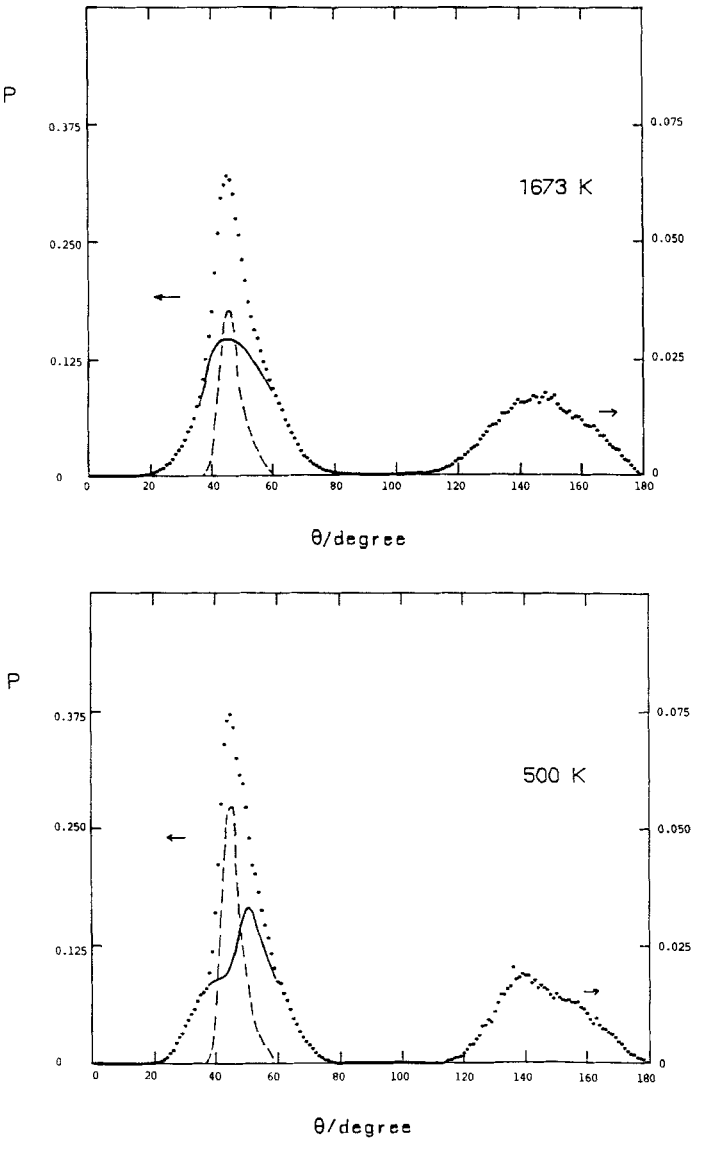

Figure 6 Angular distribution of Si_i–O–Si_j at 1673 K and 500 K. The distribution above 100 is drawn on an expanded scale (× 5). The solid and broken lines show the component for oxygens connecting with neither Si_i nor Si_j and that for oxygens connecting with either Si_i or Si_j, respectively.

as well as a single peak at 500 K. This suggests that at low temperature oxygen atoms would occupy some local energy-minimum sites, the motion between which is restricted.

The orientations of the O*–Si* bond with reference to the SiO_4 unit sharing the O* atom may be classified into 2 types, α- and β-types, which are shown in Figure 7(a); the criteria for the classification are given in the legend of Figure 7(a). As seen from Table 5, the abundances of α- and β-types are nearly equal independently of temperature.

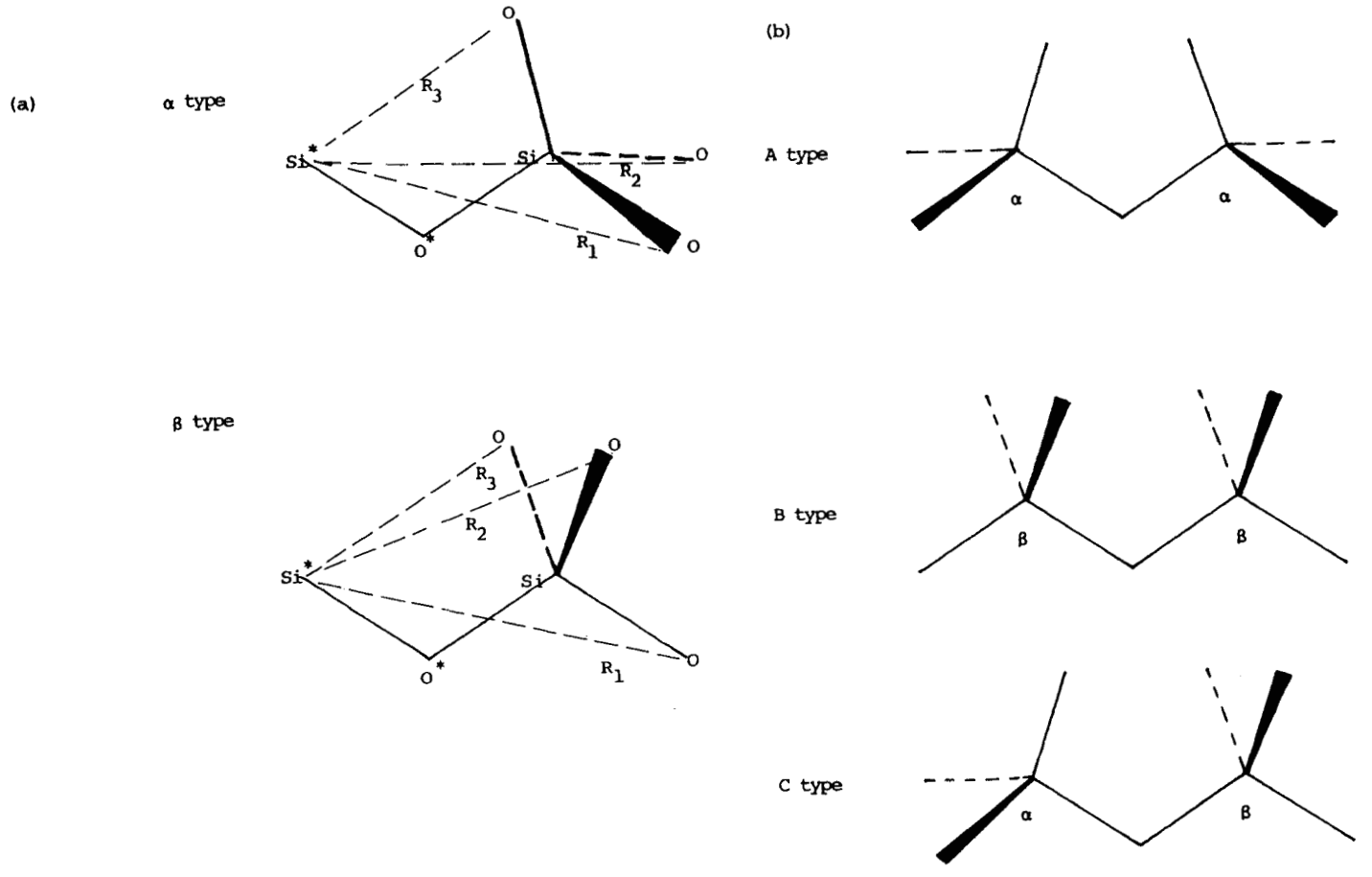

Figure 7 Typical local structures of connection of SiO_4 units. (a) α type: R2 > (R1 + R3)/2 and β type: R2 ⩽ (R1 + R3)/2; (R1 ⩾ R2 ⩾ R3). (b) A(α, α) type, B (β, β) type and C (α, β) type.

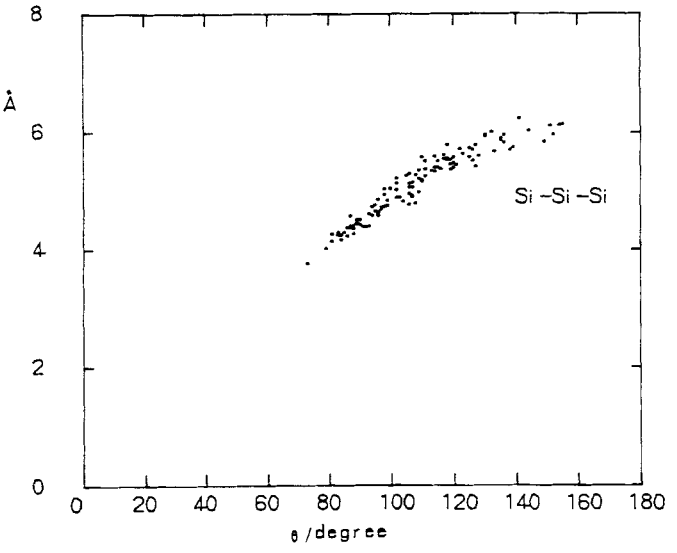

Figure 8 Relationship between distance Si_i–Si_k and angle $\angle Si_i$–Si_j–Si_k at an arbitrarily chosen step at 1673 K.

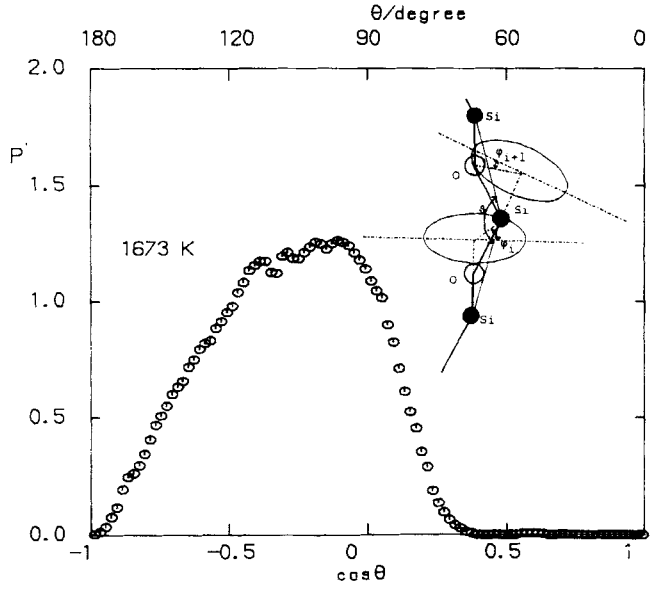

Figure 9 Distribution of the angle $\angle$ Si–Si–Si at 1673 K, 973 K and 500 K. For 973 K, the results of other series of runs are given in (b) and (c). (b): cooling schedule is same as that in (a) and initial configuration of atoms is different with that in (a). (c): initial configuration of atoms is same as in (b) and cooling rate is faster than those in (a) and (b) ($\sim 2 \times 10^5$ K/s). In every case, we can observe some distinct peaks, although a detail of distribution pattern depends on both of the configuration and the cooling rate. For example, the angle at 60° observed in (a) corresponds that structure,

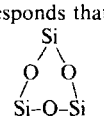

shown in Figure 5 which was developed during slower cooling process, while the original angles at 1673 K seems to be preserved at faster cooling rate. Definitions of the angle $\angle$ Si–Si–Si, θ, and the rotation angle, ϕ_i, are shown in the inset.

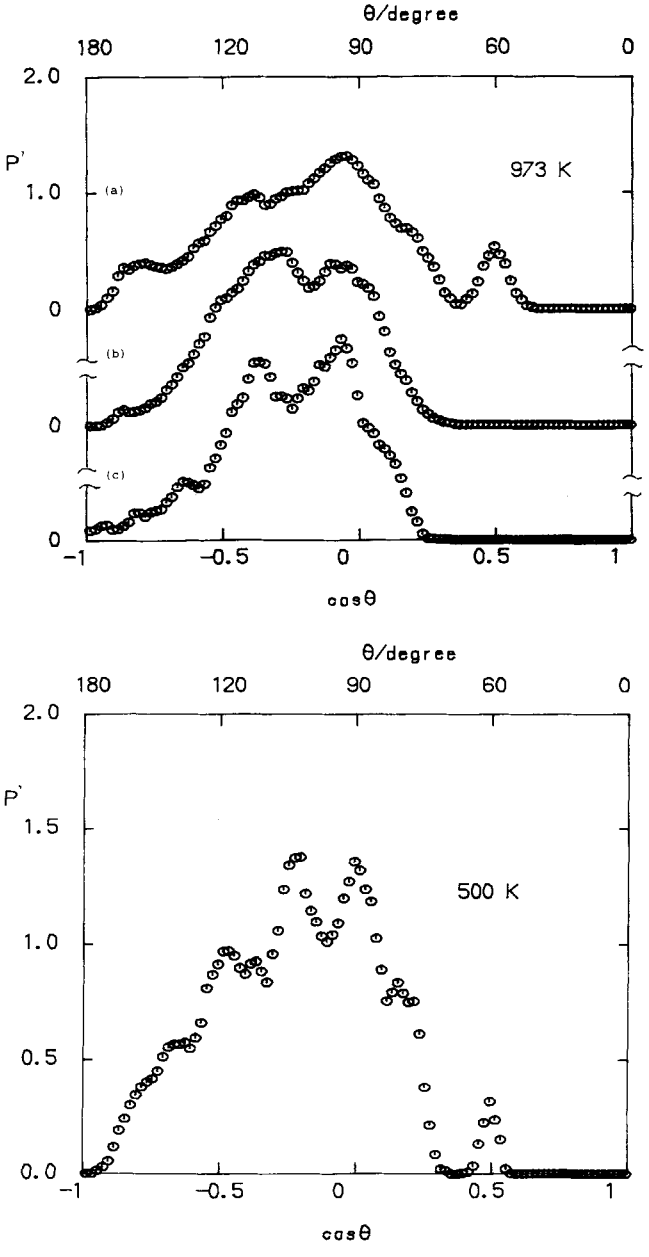

Figure 9 Cont.

The relative orientations of two neighboring SiO_4 units are classified into 3 types $A(\alpha, \alpha)$, $B(\beta, \beta)$ and $C(\alpha, \beta)$ as shown in Figure 7(b). The abundances are given also in Table 5. The abundance of C is largest among the three types at each temperature. The abundance of type C is slightly larger than expected from a random combination

Table 5 Abundance of local structure types

T/K	*Type*	
	α	β
1673	48.9%	51.1%
1173	50.7%	49.3%
973	48.4%	51.6%
700	49.0%	51.0%
500	51.2%	48.8%

T/K	*Type*		
	A	*B*	*C*
1673	23.2%	25.4%	51.4%
	(23.9%	26.1%	50.0%)*
1173	24.1%	22.7%	53.3%
	(25.7%	24.3%	50.0%)*
973	22.8%	26.0%	51.2%
	(23.4%	26.8%	49.9%)*
700	23.0%	25.0%	52.0%
	(24.0%	26.0%	50.0%)*
500	23.6%	21.3%	55.0%
	(26.2%	23.6%	50.0%)*

* The values in parentheses are the expected values from a random combination of α- and β-types.

of the types α and β, whereas those of type *A* and *B* are smaller. In the glassy state, the structural changes among them are restricted. In passing, in the Li_2SiO_3 crystal type *C* is dominant.

3.2.2 *Splittings of the second peak of $g_{Si-Si}(r)$ and of the angular distributions $\angle$ Si–Si–Si*

A nearly linear relationship is found between the distance $Si_{i'}$–$Si_{k'}$ and the $\angle Si_{i'}$–$Si_{j'}$–$Si_{k'}$, where $Si_{i'}$ and $Si_{k'}$ are neighbored to $Si_{j'}$ within the r_{min} for $g_{Si-Si}(r)$.

As an example, the relation at an arbitrarily chosen step at 1673 K is shown in Figure 8. Thus, the splittings found for the second peak of g_{Si-Si} correspond to the several distinct preferential values of the angle. The angular distribution functions $P'(\cos\theta)$ defined by Equation (3) for $\angle Si_{i'}$–$Si_{j'}$–$Si_{k'}$ at 1673 K, 973 K, 500 K are shown in Figure 9.

$$P'(\cos\theta) = C'\, dn(\cos\theta)/d\cos\theta \tag{3}$$

where $dn(\cos\theta)$ is the number of the triplets in which $\angle Si_{i'}$–$Si_{j'}$–$Si_{k'}$ is between $\cos\theta$ and $\cos\theta + d\cos\theta$; C' is a normalization constant taken so that $\int_{-1}^{1} P'(\cos\theta)\, d\cos\theta = 1$. At 1673 K, the $P'(\cos\theta)$ has a broad peak at 100°–120°, whereas at lower temperature some distinct peaks appear. The time evolution of arbitrarily chosen angles $\angle Si_{i'}$–$Si_{j'}$–$Si_{k'}$ is shown in Figure 10(a) for 1673 K, and Figure 10(b) for 500 K. Figure 10(a) shows that at this temperature the angle $\angle Si_{i'}$–$Si_{j'}$–$Si_{k'}$ varies rapidly.

Some distinct peaks for the angle at lower temperature shown in Figure 9 are attributable to the finding that the angle ϕ_i defined in the inset of Figure 9 is nearly frozen on cooling. This corresponds to the finding that local structures *A*, *B*, and *C*

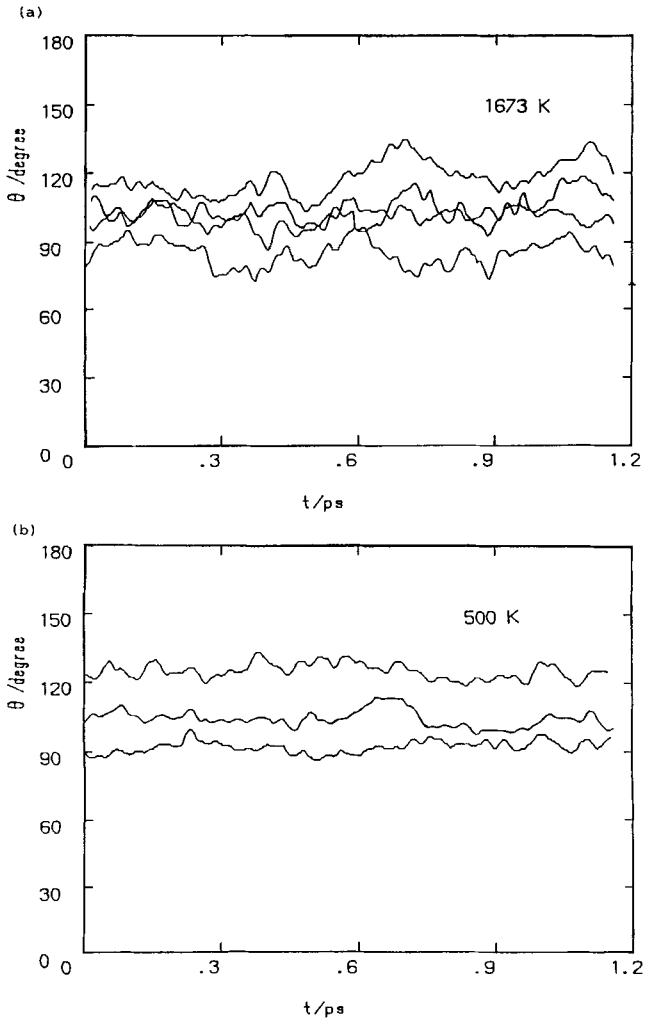

Figure 10 Time evolution of arbitrarily chosen Si–Si–Si angles. (a): 1673 K, (b): 500 K.

have relatively long life time at low temperature. Then some conformers made of such structures with restricted values of ϕ_i exist in the glassy state.

Splittings of the peak of ∠ Si–Si–Si are found even at 973 K where the system seems to be in the super-cooled liquid state. In MD simulations of Lennard–Jones and hard-sphere fluids, clear splittings of the second peak in $g(r)$ have been observed [12, 13]. This feature has been discussed in connection to hard sphere amorphous close packing, although it cannot distinguish between the glassy and liquid states [4].

Also in the present system like in the monoatomic systems, the existence of splittings does not necessarily distinguish between the liquid and glassy states; however, the splittings appear as a result of the fairly restricted motion of chains, and may be regarded as a forerunning phenomenon of glass transition.

4 CONCLUSION

Some structural changes in the short and medium range at around the glass transition temperature were observed. When the molten Li_2SiO_3 system was cooled down in MD simulation, not only the translational motion of the atoms but also the internal rotational motion of the chains became restricted even above the glass transition point. The splittings in the second peak of $g_{Si-O}(r)$, $g_{Si-Si}(r)$ and the corresponding angular correlation of $\angle$ Si–O–Si, $\angle$ Si–Si–Si in the glassy state suggest that restricted relative orientations of the neighboring SiO_4 units anticipate the glass transition.

The analysis of coordination polyhedra of oxygens about an Li^+ ion is also useful for understanding the glass transition [8]. A further study is necessary on the effects of the limited size of the MD cell, the cooling rate, the covalency of the bond and the deviation from pairwise additivity of the potentials, as the glass transition in real systems may be affected by these factors.

Acknowledgements

A part of the calculations in this work were performed with HITAC M-680 and S-820 at the Institute for Molecular Science at Okazaki. The CPU time made available is gratefully acknowledged. The expenses of this work were defrayed partly be the Grant for the Encouragement of Young Scientists No. 03740311 from the Ministry of Education, Science and Culture, Japan. We thank Dr. K. Kawamura for providing the MD program for crystals.

References

[1] K. Furuhashi, J. Habasaki and I. Okada, "A molecular dynamics study of structures and dynamic properties of molten $NaBeF_3$ and Na_2BeF_4", *Mol. Phys.*, **59,** 1329 (1986).
[2] Y. Ida, "Interionic repulsive force and compressibility of ions", *Phys. Earth Planet. Interiors*, **13,** 97 (1976).
[3] Y. Waseda and H. Suito, "The structure of molten alkali metal silicates", *Trans. ISIJ*, **17,** 82 (1977).
[4] M. Takahashi, H. Toyuki, M. Tatsumisago and T. Minami, "X-ray diffraction studies of rapidly quenched Li_2O–SiO_2 glasses", *Chemistry Express*, **13,** 17 (1988).
[5] M. Misawa, D.L. Price and K. Suzuki, "The short-range structure of alkali disilicate glasses by pulsed neutron total scattering", *J. Non-Cryst. Solids*, **37,** 85 (1980).
[6] L.V. Woodcock, "Isothermal molecular dynamics calculations for liquid salts", *Chem. Phys. Lett.*, **10,** 257 (1971).
[7] J.O'M. Bockris, J.W. Tomlinson and J.L. White, "The structure of the liquid silicates", *Trans. Faraday Soc.*, **52,** 299 (1956).
[8] J. Habasaki, "Molecular-dynamics study of glass formation in the Li_2SiO_3 system", *Mol. Phys.*, **70,** 513 (1990).
[9] T.F. Soules and R.F. Busbey, "Sodium diffusion in alkali silicate glass by molecular dynamics", *J. Chem. Phys.*, **75,** 969 (1981).
[10] J. Habasaki, I. Okada and Y. Hiwatari, to be published.
[11] M. Tatsumisago, T. Minami and M. Tanaka, "Glass formation by rapid quenching in lithium silicates containing large amounts of Li_2O", *Jpn. J. Cer. Soc.* **93,** 581 (1985).
[12] J.L. Finney, "Random packings and the structure of simple liquids", *Proc. Roy. Soc. A*, **319,** 479 (1970).
[13] C.H. Bennett, "Serially deposited amorphous aggregates of hard spheres", *J. Appl. Phys.*, **43,** 2727 (1972).
[14] A. Rahman, M.J. Mandell and J.P. McTague, "Molecular dynamics study of an amorphous Lennard-Jones system at low temperature", *J. Chem. Phys.*, **64,** 1564 (1976).

APPENDIX

Other details of methodology of calculation are as follows. The periodic cube contains 144 Li, 72 Si and 216 O atoms. The coulombic energy is calculated using the Ewald summation. The cut distance in real space was L/2 and the reciprocal lattice vectors $|n|^2$ were counted up to 27, which corresponds to 309 vectors. The equations of motion were integrated *via* a Verlet scheme.

Check of the Potential Model

The potential parameters used in this work were obtained by modifying the MAM potential and checked against the crystal structure of Li_2SiO_3. The space group is $Cmc2_1$. The number of atoms in the basic cell is 432. The ideal positions of the crystal structure of Li_2SiO_3 were used as the starting positions of all the atoms. The initial configuration has been retained after a run of more than several thousands time steps (time step is 2 fs) at constant temperature (300 K).

The atomic coordinates of the structure obtained are as follows, those for experimental ones (Von H. Seemann, *Acta Cryst.*, **8**, 251 (1956)) being given in parentheses:

Atom	*Position*	*x*	*y*	*z*
Li	(8b)	0.171(0.160)	0.334(0.320)	−0.021(0.000)
Si	(4a)	0.000(0)	0.169(0.164)	0.501(0.537)
O(1)	(8b)	0.139(0.141)	0.311(0.321)	0.412(0.450)
O(2)	(4a)	−0.001(0)	0.103(0.100)	0.841(0.860)